Preprints.org

Article

Not peer-reviewed version

Series Solution and Its Extension for the Nonlinear Flow Response of Soft Hair Beds

Bo Hua Sun *, Bo Pang , Meng Li

Posted Date: 6 August 2024

doi: 10.20944/preprints202408.0074.v1

Keywords: soft hair beds; Stokes flow; series solution; perturbation solution

Preprints.org is a free multidiscipline platform providing preprint service that is dedicated to making early versions of research outputs permanently available and citable. Preprints posted at Preprints.org appear in Web of Science, Crossref, Google Scholar, Scilit, Europe PMC.

Copyright: This is an open access article distributed under the Creative Commons Attribution License which permits unrestricted use, distribution, and reproduction in any medium, provided the original work is properly cited.

Preprints.org (www.preprints.org) | NOT PEER-REVIEWED | Posted: 6 August 2024 doi:10.20944/preprints202408.0074.v1

Disclaimer/Publisher's Note: The statements, opinions, and data contained in all publications are solely those of the individual author(s) and contributor(s) and not of MDPI and/or the editor(s). MDPI and/or the editor(s) disclaim responsibility for any injury to people or property resulting from any ideas, methods, instructions, or products referred to in the content.

Article

Series Solution and Its Extension for the Nonlinear Flow Response of Soft Hair Beds

Bo Hua Sun [1,2] Bo Pang [2,3] and Meng Li [2,3]

[1] Beijing Institute of Nanoenergy and Nanosystems, Chinese Academy of Sciences, Beijing 101400, China
[2] Institute of Mechanics and Technology Xian University of Architecture and Technology, Xian 710055, China
[3] Xian University of Architecture and Technology, Xian 710055, China
* Correspondence: sunbohua@xauat.edu.cn

Abstract: In nature and engineering applications, flexible fiber beds covering biological surfaces can play a role in reducing resistance. These fibers deform under the action of fluids, and this deformation affects the fluid flow state, forming a complex fluid-solid interaction phenomenon. To quantitatively analyze such issues, the physical model is simplified to the deformation problem of an soft hair bed caused by Stokes flow, and the deformation problem of a single fiber caused by Stokes flow is further studied. The deformation problem of an elastic single fiber in a channel caused by Stokes flow can be described by a nonlinear integral equation. We have obtained a new series solution, which has been compared with the previous perturbation method to verify the accuracy and effectiveness of the series solution. Meanwhile, we have further provided an extended form of flexible fiber deformation through experimental fitting. This fluid-solid interaction problem involves multiple fields and is very important in many natural and engineering systems. The research in this paper can not only help us better understand complex phenomena in nature but also delve into the interaction mechanism between fluids and solids, providing a theoretical basis for future scientific research and engineering applications.

Keywords: soft hair beds; Stokes flow; series solution; perturbation solution

1. Introduction

Deformable fiber structure has a very wide range of applications on both micro and macro scales. The flexible hair bed structure in living organisms is widely present in a variety of tissues and organs. A viscoelastic cytoskeleton composed of actin filaments and myosin motors, which can produce general contraction motion, exert force and actively drive cell shape changes [1–4]. The cilia system of mammalian respiratory tract is the body 's defense mechanism, which can help to remove mucus and foreign body [5]. Aquatic organisms such as Paramecium and some protozoans use cilia to move [6], which gives cells motor and sensory functions [7–11]. The primary cilia in the central nervous system react as mechanical sensors to help cell-to-cell material exchange and signal transmission and regulate the central nervous system [12,13]. The flagella present in some single-cell organisms such as bacteria and multicellular organisms such as some worms and flagella act as a mobile organ [14–16]. When the flagella are driven synchronously, the dynamic interaction between them and the fluid can make the cells swim faster [17]. The flexible filaments of dandelion seeds diffuse and deform during flight, thereby reducing their flow resistance in the air [18–22]. These flexible fiber bed structures under the action of fluid are important components of organisms to adapt to the environment and complete specific functions, which are of great significance for maintaining tissue structure and function and regulating cell behavior. Studying their motion and structural changes in fluids is a key part of the intersection of mechanics and biology and also helps to understand the relationship between the microstructure and mechanical function of organisms.

With the increasing interest in the study of flexible fibers interacting with fluids, many studies have found that when deformable solids interact with fluid viscosity effects, a rich nonlinear behavior will be generated [23–25]. Imitating this structure can be applied to the design of bionic robots [26,27], underwater robots and micro-nano devices, which is of great significance in the fields of biology, engineering and physics.

© 2024 by the author(s). Distributed under a Creative Commons CC BY license.

Preprints.org (www.preprints.org) | NOT PEER-REVIEWED | Posted: 6 August 2024 doi:10.20944/preprints202408.0074.v1

According to the previous research hypothesis of Alvarado et al. [28], the deformation of the hairs in the channel under the action of shear-driven Stokes flow is simplified as a nonlinear problem, in which the small parameter perturbation analysis method is used to solve the problem numerically. We found that the solution of the hair bed height obtained by the perturbation method has a certain scope of application, which can only describe the fluid flow problem with very small velocity. In the perturbation analysis, only the first-order and second-order effects of small parameters (when $\epsilon < 1$) are considered, which may lead to the inability to describe the physical problems of the elastic hair bed system more comprehensively and accurately. Therefore, based on the research of Alvarado et al. [28], we have tried and explored a series solution to the deformation problem of flexible fibers under shear flow to extend the domain of the small parameter (when $\epsilon < 2$).

2. Mathematical model of the problem

Alvarado et al.[28] developed a model system of elastomer hairs immersed in high-viscosity fluids to study the effect of fluid flow on hairs deformation, as shown in Figure 1. The elastomer hairs is covered on a fixed plane surface, immersed in the fluid, and faces a smooth surface moving at a speed of $v\vec{e}_x$, with a distance H between the two planes, measured from the bottom of the hair $z = 0$. On the moving surface, the no-slip boundary condition remains unchanged. The model assumes that the fluid velocity at the top of the hair is zero, and the hair is subjected to the shear stress of the fluid.

The influence of elastic-plastic coupling on the system resistance response is characterized by introducing a region-specific impedance, which is defined as

$$Z(v) = \frac{\tau(v)}{v} = \frac{\eta}{H - h(v)}. \tag{1}$$

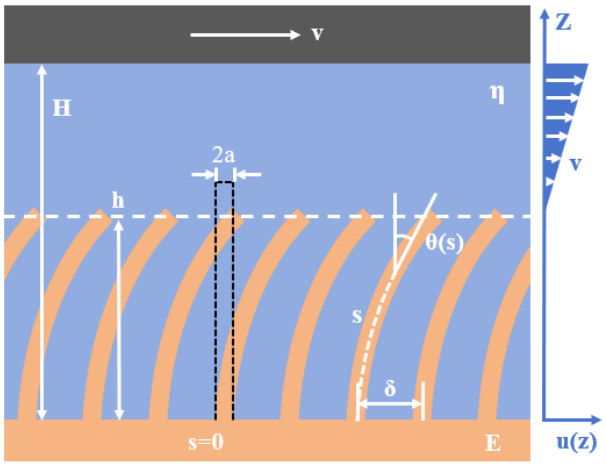

Figure 1. The schematic diagram of the system model of the coupling of deformable hairs and Stokes flow

Based on the above model, this paper refers to the simplification of Alvarado et al. [28] , and considers the immersed slender hair as an Euler-Bernoulli elastic beam. In the fluid mechanics equation, the acceleration term in the Navier-Stokes equation is removed, leaving the velocity term to solve the simplified model.

$$\begin{aligned} \nabla p - \eta \Delta v &= 0, \\ \nabla \cdot v &= 0, \end{aligned} \tag{2}$$

where v is the fluid velocity, p is the pressure, and η is the viscosity of the fluid.

Preprints.org (www.preprints.org) | NOT PEER-REVIEWED | Posted: 6 August 2024 doi:10.20944/preprints202408.0074.v1

According to the large deformation theory of beam [29–31], the Euler Elastica equations are expressed as

$$\begin{aligned} EI\frac{d\theta}{ds} + Q &= 0, \\ \frac{dz}{ds} &= \cos\theta, \\ \frac{dx}{ds} &= \sin\theta, \end{aligned} \tag{3}$$

where E is the Young 's modulus of the elastic fiber, I is the cross-section moment of inertia of the elastic fiber, M is the bending moment, and Q is the shear force.

Taking into account the effect of fluid shear stress, and using the relationship $\tau = \eta/(H - h(v))$, the shear stress Q acting on the fiber can be expressed as

$$Q = \frac{\pi a^2}{\phi}\tau\cos\theta = \frac{\pi a^2}{\phi}\frac{\eta}{H - h(v)}\cos\theta, \tag{4}$$

among them, ϕ is the area ratio of the fiber, a is the radius of the fiber, L is the length of the fiber ,h is the height of the fiber, that is, the position of the tip plane $h(\theta(\xi)) = \int_0^L \cos\theta(\xi)ds$. After the equation 4 is substituted into the equation 3, the equilibrium calculus equation of the system is obtained as follows

$$EI\frac{d^2\theta(s)}{ds^2} + \frac{\pi a^2}{\phi}\frac{\eta v\cos\theta(s)}{H - \int_0^L \cos\theta(s)ds} = 0. \tag{5}$$

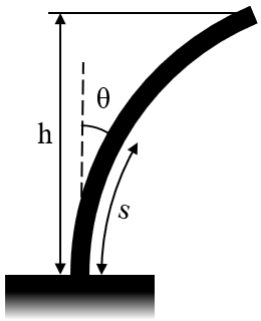

Figure 2. A schematic diagram of single fiber bending

The dimensionless parameter $\xi = s/L$ is introduced, and ξ is differentiated on both sides at the same time, which can be dimensionless as $ds = Ld\xi$, $d^2\theta/ds^2 = d^2\theta/L^2d\xi^2$, $\int_0^L \cos\theta ds = \int_0^1 \cos\theta L d\xi = L\int_0^1 \cos\theta d\xi$, substituting it into the equilibrium differential equation, we get

$$\frac{d^2\theta}{L^2d\xi^2} + \frac{4\eta v}{Ea^2\phi}\frac{\cos\theta}{H - L\int_0^1 \cos\theta d\xi} = 0. \tag{6}$$

Here we introduce $\lambda = L/H$, $\epsilon = 4\eta L^2 v/(Ea^2\phi H)$, the height of the fiber can be dimensionless to $\hat{h} = \int_0^1 \cos\theta d\xi$, and the and the impedance is rescaled as $\hat{Z} = (h/H)(H - L)/(H - h) = \hat{h}(1 - \lambda)/(1 - \lambda\hat{h})$, the equilibrium differential equation can be dimensionless

$$\frac{d^2\theta}{d\xi^2} + \epsilon\frac{\cos\theta}{1 - \lambda\int_0^1 \cos\theta d\xi} = 0. \tag{7}$$

In the following, we only consider the special case of straight fibers perpendicular to the anchoring surface, which means that the initial angle is zero, that is, $\theta_0 = 0$, and the fiber model in this case

Preprints.org (www.preprints.org) | NOT PEER-REVIEWED | Posted: 6 August 2024 doi:10.20944/preprints202408.0074.v1

simplifies the analysis. The bottom end of the fiber is fixed, so $\theta|_{\xi=0} = 0$; the boundary condition at the free end is $\theta'|_{\xi=1} = 0$, indicating that the curvature of the fiber is continuous at the free end.

However, directly solving this integro-differential equation, i.e., equation 7, is often a great challenge, especially when curvature constraints at the free end are involved, which may lead to nonlinear behavior and complex solutions. Alvarado et al. [28] proposed an innovative method in their research, that is, using a small parameter perturbation technique. Through perturbation analysis, the problem is decomposed into a series of approximate problems that are easier to deal with, and then these approximate problems are solved step by step. Finally, an approximate solution of fiber deformation with respect to velocity is obtained, which provides a very valuable physical insight and theoretical guidance for our related research.

3. Series Solution of Fiber Deformation

We approximate the equilibrium differential equation of the system by calculating the third order of the dimensionless velocity ξ

$$\theta(\xi) = \Sigma a_n \xi^n \approx a_0 + a_1\xi + a_2\xi^2 + a_3\xi^3, \tag{8}$$

where a_n is the function to be determined.

Substituting $\theta(\xi)$ into the boundary conditions, $a_0 = 0$ and $a_1 = -2a_2 - 3a_3$ are obtained. In this way, θ can be expressed and $\cos\theta$ can be expanded in series.

$$\theta(\xi) = \Sigma a_n \xi^n \approx (-2a_2 - 3a_3)\xi + a_2\xi^2 + a_3\xi^3, \tag{9}$$

at the same time

$$\begin{aligned} \cos\theta &= \Sigma(-1)^k \tfrac{\theta^{2k}}{(2k)!} \approx 1 - \tfrac{\theta^2}{2} + \tfrac{\theta^4}{24} \\ &= 1 - \tfrac{1}{2}[(-2a_2 - 3a_3)\xi + a_2\xi^2 + a_3\xi^3]^2 \\ &\quad + \tfrac{1}{24}[(-2a_2 - 3a_3)\xi + a_2\xi^2 + a_3\xi^3]^4. \end{aligned} \tag{10}$$

Substituting these two expressions into the equation, the zero to first-order coefficient equations of ξ are extracted respectively, and the simultaneous solution is obtained $a_1 = \epsilon + \lambda\epsilon/2$, $a_2 = -\epsilon/2$, $a_3 = -\lambda\epsilon/6$, In this way, we can easily get the series solution of θ as follows

$$\theta(\xi) = \Sigma a_n \xi^n \approx (\epsilon + \frac{1}{2}\lambda\epsilon)\xi + (-\frac{1}{2}\epsilon)\xi^2 + (-\frac{1}{6}\lambda\epsilon)\xi^3. \tag{11}$$

The position of the tip plane of the flexible fiber, that is, the height of the dimensionless fiber $\hat{h}$, can be solved by taking the cosine function and then integrating the above formula

$$\begin{aligned} \hat{h} = 1 &+ (A_1\lambda^4 + A_2\lambda^3 + A_3\lambda^2 + A_4\lambda + A_5)\epsilon^4 \\ &+ (A_6\lambda^2 + A_7\lambda + A_8)\epsilon^2, \end{aligned} \tag{12}$$

and the specific value of the coefficient A_n is shown in Table 1.

Table 1. $\hat{h}$ solution function coefficient table

coefficient	value	coefficient	value
A_1	0.00018510	A_5	0.00105820
A_2	0.00264901	A_6	-0.02698413
A_3	0.00114284	A_7	-0.08472222
A_4	0.00273231	A_8	-0.06666667

Finally, the recalibrated impedance is calculated as

$$\hat{Z} = \frac{(-1+\lambda)(B_1\epsilon^2\lambda^2 + B_2\epsilon^2\lambda + B_3\epsilon^2 - B_4)}{B_4 + B_1\epsilon^2\lambda^3 + B_2\epsilon^2\lambda^2 + (B_3\epsilon^2 - B_4)\lambda}, \tag{13}$$

Preprints.org (www.preprints.org) | NOT PEER-REVIEWED | Posted: 6 August 2024 doi:10.20944/preprints202408.0074.v1

and the specific value of the coefficient B_n is shown in Table 2.

Table 2. $\hat{Z}$ solution function coefficient table

coefficient	value	coefficient	value
B_1	136	B_3	336
B_2	427	B_4	5040

4. Numerical Analysis and Discussion

We can clearly see that for the problem of nonlinear flow of flexible fiber bed, the assumption of fiber deformation has certain limitations. Because the model used in this paper has certain limitations, when ϵ is greater than 2 and the fiber bed has strong deformation, this model is no longer applicable. In order to better describe the influence of velocity on the deformation of fiber bed, we extracted the experimental data of Alvarado et al. [28], and carried out numerical analysis and processing on the obtained data.

Figure 3 shows the variation curve of the recalibrated impedance with respect to the recalibrated speed. The experimental data [28] is directly used to compare with the series analytical solution calculated by us in the range of the recalibrated speed ϵ less than 2. From Figure 3, it can be seen that the numerical solution curve is consistent with the trend of the experimental results, and the series solution obtained by comparison is closer to the experimental value and more accurate than the results obtained by perturbation analysis.

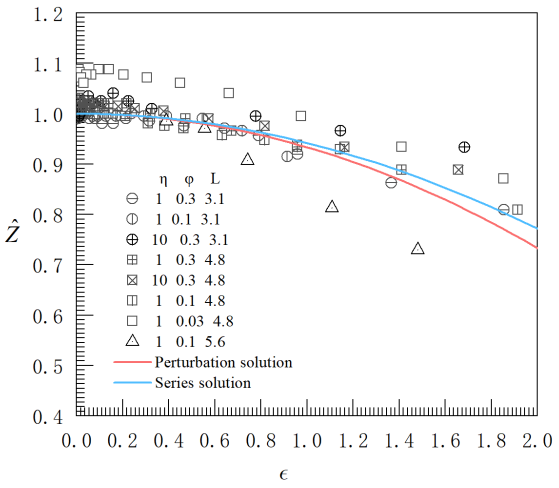

Figure 3. Comparison between series solution and perturbation solution

Since the height of the fiber in the model used in this paper cannot be lower than the surface of the anchoring plane, that is, we calculate the height of the dimensionless fiber $\hat{h} > 0$. It should be noted that the limit of $\hat{h} \longrightarrow 0$ cannot be achieved. When the flow velocity of the fluid exceeds the limit velocity, the fiber deforms very strongly when it bends to the plane surface, so we find the scope of application of this model. As shown in Figure 4, the theoretical model is divided into two parts. Part I is the series solution of the system equilibrium differential equation and part II is the extended form of the series solution obtained by data fitting.

Considering the range of heights of slender fibers, when the value is minimum, the fibers are in a collapsed state of 0, and when the value is maximum, the fibers are in an upright state of L. We have chosen a power function to fit the deformation of the fibers. The power function is a type of generalized linear model, which can be seen as a nonlinear extension of linear models, capable of capturing more complex data structures and describing nonlinear relationships between data well. Moreover, it is relatively simple in mathematical processing and can find the best parameters through

Preprints.org (www.preprints.org) | NOT PEER-REVIEWED | Posted: 6 August 2024 doi:10.20944/preprints202408.0074.v1

methods like least squares to achieve a higher degree of fit. Alvarado et al. [28] predicted strong deformation fibers as $\hat{Z} \sim v^{-1/2}$ in their article. Here, through parameter fitting, we provide the exact expression for it

$$\hat{Z} = C_1 \epsilon^{C_2}. \tag{14}$$

Through a series of data processing, we obtained $C_1 = 1.1127$ and $C_2 = -0.484$. Equation 14 represents the fitting parameter expression for region II.

$$\hat{Z} = \begin{cases} \frac{(-1+\lambda)(B_1\epsilon^2\lambda^2+B_2\epsilon^2\lambda+B_3\epsilon^2-B_4)}{B_4+B_1\epsilon^2\lambda^3+B_2\epsilon^2\lambda^2+(B_3\epsilon^2-B_4)\lambda}, & 0 < \epsilon < 2 \\ 1.112\epsilon^{-0.48}, & \epsilon > 2. \end{cases} \tag{15}$$

Equation 15 represents the overall expanded expression of the impedance for the re-calibrated elastic fiber bed with respect to the re-calibrated velocity. Additionally, in accordance with the prediction $\hat{Z} \sim v^{1/2}$ proposed by Alvarado et al. [28], we fitted the coefficient $C_3 = 1.091754444$ and provided the specific expression for this part

$$\hat{Z} = 1.09175\epsilon^{-1/2}, \qquad \epsilon > 2. \tag{16}$$

From Figure 5, it can be seen that the overall trend of the numerical solution curve is in agreement with the experimental results. By transforming the coordinates, we obtained two fitting curves for comparison with the experimental data.

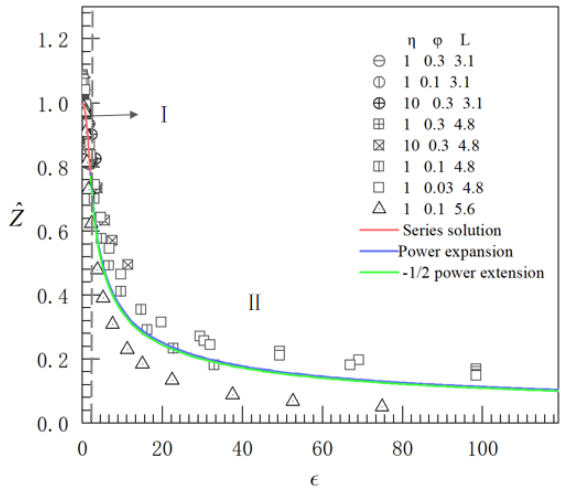

Figure 4. The comparison between the analytical solution and the experimental value

When the fluid velocity is high, the fibers may undergo significant deformation, which warrants further investigation. The model assumed in this paper is relatively simple, so we have introduced a new topic here to explore this new issue in depth. This aims to discover and conduct in-depth research on this new problem, providing new ideas and directions for future research work.

Preprints.org (www.preprints.org) | NOT PEER-REVIEWED | Posted: 6 August 2024 doi:10.20944/preprints202408.0074.v1

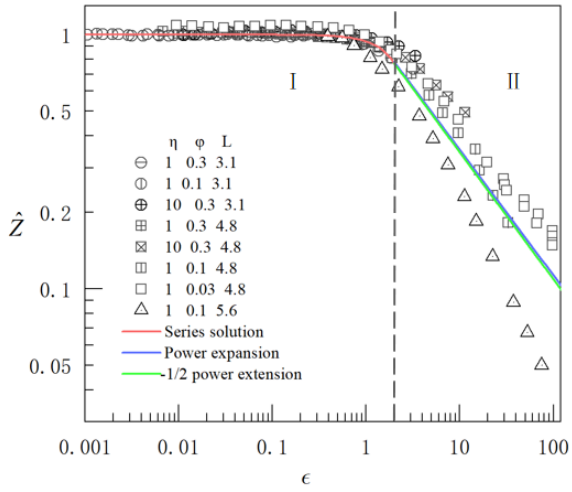

Figure 5. The comparison between the analytical solution and the experimental value in logarithmic coordinates

5. Conclusion

In this paper, based on the model of Alvarado et al. [28], we use the numerical method of series expansion to obtain a new analytical solution of the differential equation of hair deformation immersed in shear flow through more accurate calculation, and find that the model has a certain scope of application. Through further calculations, we verify that the solution with second-order or higher accuracy cannot improve this theoretical model.

Then, the analytical solution obtained by us is compared with the experimental value. The numerical solution is in good agreement with the experimental value within the scope of application of the model, which can better describe the deformation of the hair. However, when the flow velocity is too large, due to the limitations of the theoretical model, there is no way to achieve strong deformation when the hair bends to the surface. Therefore, we further fit the experimental data and give the fitting formula when the hair undergoes strong deformation as an extended form of the series solution.

In future work, consider selecting a more suitable model to delve deeper into this matter and broaden the investigation with additional numerical simulations.

Conflicts of Interest: The authors declare that there are no competing financial interests.

Data Availability Statement: The data supporting the findings of this study are available from the corresponding author upon reasonable request.

References

1. Brangwynne C P, Koenderink G H, MacKintosh F C, et al. Cytoplasmic diffusion: molecular motors mix it up. The Journal of cell biology, 2008, 183(4): 583-587.
2. Weber S C, Spakowitz A J, Theriot J A. Nonthermal ATP-dependent fluctuations contribute to the in vivo motion of chromosomal loci. Proceedings of the National Academy of Sciences, 2012, 109(19): 7338-7343.
3. Gunning P W, Ghoshdastider U, Whitaker S, et al. The evolution of compositionally and functionally distinct actin filaments. Journal of cell science, 2015, 128(11): 2009-2019.
4. Alvarado J, Sheinman M, Sharma A, et al. Force percolation of contractile active gels. Soft matter, 2017, 13(34): 5624-5644.
5. Role of Cilia, Mucus, and Airway Surface Liquid in Mucociliary Dysfunction: Lessons from Mouse Models Marcus A. Mall Journal of Aerosol Medicine and Pulmonary Drug Delivery 2008 21:1, 13-24
6. Bouhouche, K., Valentine, M.S., Le Borgne, P., Lemullois, M., Yano, J., Lodh, S., Nabi, A., Tassin, A.M., Van Houten, J.L., 2022. Paramecium, a Model to Study Ciliary Beating and Ciliogenesis: Insights From Cutting-Edge Approaches. Frontiers in Cell and Developmental Biology 10.

Preprints.org (www.preprints.org) | NOT PEER-REVIEWED | Posted: 6 August 2024 doi:10.20944/preprints202408.0074.v1

7. Bengueddach H., Lemullois M., Aubusson-Fleury A., Koll F. (2017). Basal Body Positioning and Anchoring in the Multiciliated Cell Paramecium Tetraurelia: Roles of OFD1 and VFL3. Cilia 6, 6.
8. Bloodgood R. A. (2010). Sensory Reception Is an Attribute of Both Primary Cilia and Motile Cilia. J. Cel Sci 123, 505–C509.
9. Bonini N., Nelson D. (1988). Differential Regulation of Paramecium ciliary Motility by cAMP and cGMP. J. Cell. Biol. 106, 1615–C1623.
10. Brooks E. R., Wallingford J. B. (2014). Multiciliated Cells. Curr. Biol. 24, R973–CR982.
11. Guemez-Gamboa, A., Coufal, N.G., Gleeson, J.G., 2014. Primary Cilia in the Developing and Mature Brain. Neuron 82, 511–C521.
12. Lee, Ji E; Gleeson, Joseph G. Cilia in the nervous system: linking cilia function and neurodevelopmental disorders. Current Opinion in Neurology 24(2):p 98-105, April 2011.
13. Berbari N F, O'Connor A K, Haycraft C J, et al. The primary cilium as a complex signaling center. Current Biology, 2009, 19(13): R526-R535.
14. Carvalho-Santos Z., Azimzadeh J., Pereira-Leal J. B., Bettencourt-Dias M. (2011). Tracing the Origins of Centrioles, Cilia, and Flagella. J. Cel Biol 194, 165–C175.
15. Fassad M. R., Shoemark A., le Borgne P., Koll F., Patel M., Dixon M., et al. (2018). C11orf70 Mutations Disrupting the Intraflagellar Transport-dependent Assembly of Multiple Axonemal Dyneins Cause Primary Ciliary Dyskinesia. Am. J. Hum. Genet. 102, 956–C972.
16. Quarmby L. M. (2004). Cellular Deflagellation. Int. Rev. Cytol. 233, 47–C91.
17. Hu, S.; Meng, F. Multiflagellate Swimming Controlled by Hydrodynamic Interactions. Phys. Rev. Lett. 2024, 132 (20), 204002.
18. V. Iyer, H. Gaensbauer, T. L. Daniel, and S. Gollakota, Wind dispersal of battery-free wireless devices, Nature 603, 427–C433 (2022).
19. B. H. Sun and X. L. Guo, Aerodynamic shape and drag scaling law of a flexible fibre in a flowing medium, Theor. Appl. Mech. Lett. 13, 100397 (2023).
20. B. H. Sun and X. L. Guo, Drag scaling law and parachute terminal velocity of the dandelion, AIP Adv. 13(8), 085305 (2023)
21. C. Cummins, M. Seale, A. Macente, D. Certini, E. Mastropaolo, I. M. Viola, and N. Nakayama, A separated vortex ring underlies the flight of the dandelion, Nature 562, 414–C418 (2018).
22. P. G. Ledda, L. Siconolfi, F. Viola, S. Camarri, and F. Gallaire, Flow dynamics of a dandelion pappus: A linear stability approach, Phys. Rev. Fluids 4, 071901 (2019).
23. Duprat, C., Proti, re, S., Beebe, A. Y., Stone, H. A. Wetting of flexible fibre arrays. Nature 482, 510–C513 (2012).
24. Saintyves, B., Jules, T., Salez, T. Mahadevan, L. Self-sustained lift and low friction via soft lubrication. Proc. Natl Acad. Sci. USA 113, 5847–C5849 (2016).
25. Fluid-Structure Interactions in Low-Reynolds-Number Flows (eds Duprat, C., Stone, H.) (RSC Soft Matter Series, The Royal Society of Chemistry, 2016).
26. Wehner, M. et al. An integrated design and fabrication strategy for entirely soft, autonomous robots. Nature 536, 451–C455 (2016).
27. Sareh, S., Siddall, R., Alhinai, T., Kovac, M. (2017). Bio-inspired Soft Aerial Robots: Adaptive Morphology for High-Performance Flight. In: Laschi, C., Rossiter, J., Iida, F., Cianchetti, M., Margheri, L. (eds) Soft Robotics: Trends, Applications and Challenges. Biosystems Biorobotics, vol 17. Springer, Cham.
28. Alvarado, J., Comtet, J., de Langre, E., Hosoi, A.E., 2017. Nonlinear flow response of soft hair beds. Nature Physics 13, 1014–C1019.
29. Audoly, B.,Pomeau, Y . Elasticity and Geometry: From Hair Curls to the Non-linear Response of Shells (Oxford Univ. Press, 2010).
30. Gere JM, Timoshenko SP. Mechanics of Materials. Boston: PWS Publishing Company, 1997
31. Timoshenko, S. P. Strength of Materials. 3rd ed., Part I, D. Van Nostrand Company, 1955.

Disclaimer/Publisher's Note: The statements, opinions and data contained in all publications are solely those of the individual author(s) and contributor(s) and not of MDPI and/or the editor(s). MDPI and/or the editor(s) disclaim responsibility for any injury to people or property resulting from any ideas, methods, instructions or products referred to in the content.